coatings

MDPI

Article

Dynamic Strain Response of Hot-Recycled Asphalt Pavement under Dual-Axle Accelerated Loading Conditions

Jin Li [1,*], Yingyong Li [2], Chongsheng Xin [3], Haoyu Zuo [1], Ping An [4], Shen Zuo [1,*] and Peng Liu [5]

[1] School of Transportation Civil Engineering, Shandong Jiaotong University, Jinan 250357, China; 21107008@stu.sdjtu.edu.cn
[2] Highway Service Department of Shandong Provincial Transportation Service Center, Jinan 250002, China; 21107006@stu.sdjtu.edu.cn
[3] Jinan Kingyue Highway Engineering Company Ltd., Jinan 250409, China; 19011059@stu.sdjtu.edu.cn
[4] Rizhao Transportation Development Group Co., Ltd., Rizhao 276800, China; 20107044@stu.sdjtu.edu.cn
[5] School of Civil Engineering, Central South University, Changsha 410083, China; liupeng868@csu.edu.cn
* Correspondence: 204026@sdjtu.edu.cn (J.L.); 204096@sdjtu.edu.cn (S.Z.); Tel.: +86-5-(31)-8068-7989 or +86-13-67-882-4225 (J.L.)

Abstract: Accelerated pavement testing (APT) is an effective method to study the long-term performance of pavement. Therefore, the dynamic strain behavior analysis of asphalt pavement has important guiding significance in the study of pavement failure modes. To explore the dynamic response of a high-content plant-mixed hot-reclaimed asphalt mixture under a dynamic load of vehicles, a full-scale test road was paved, and ALT biaxial accelerated loading test equipment was used to simulate the dynamic loads of vehicles. Based on parameters such as axle load, temperature, speed, and loading times, the development law for the bottom strain of the three pavement structures was analyzed. The test results show that the most unfavorable position of the asphalt pavement load is located just below the centerline of the wheel track on one side, and the damage effect of a single double-axle wheel load is far greater than that of two single-axle wheel loads. Then, the longitudinal tensile strain of the pavement bottom always maintains the alternating state of compression-tension and compression. The longitudinal tensile strain of the pavement bottom is larger than the transverse tensile strain, and transverse fatigue cracks appear first. Under normal temperature conditions, the bottom tensile strains of the three composite pavement structures under different axial loads are close, and the pavement performance of the hot-recycled asphalt pavement of structure A and structure B can meet the specification requirements. The relationship between the bottom strain and axle load is nonlinear and is directly related to the tire ground pressure, and the difference in the tensile and compressive strain values of the bottom of the three composite pavement structures is small. Under high temperature conditions, the bottom layer temperature of structure A and structure B is lower than that of structure C, and the thermal heat transfer efficiency of hot-recycled asphalt pavement is lower than that of ordinary asphalt pavement. Additionally, the longitudinal tensile strain is about 1–1.5 times that of the transverse tensile strain. Based on the Boltzmann function, the accumulative tensile strain prediction model was established to reflect the relationship between the cumulative strain at the bottom and the number of loads.

Keywords: road engineering; hot-recycled asphalt pavement; dual-axle accelerated loading; dynamic response of strain

Citation: Li, J.; Li, Y.; Xin, C.; Zuo, H.; An, P.; Zuo, S.; Liu, P. Dynamic Strain Response of Hot-Recycled Asphalt Pavement under Dual-Axle Accelerated Loading Conditions. *Coatings* **2022**, *12*, 843. https://doi.org/10.3390/coatings12060843

Academic Editor: Andrea Simone

Received: 8 May 2022
Accepted: 10 June 2022
Published: 16 June 2022

1. Introduction

The vehicle dynamic load is one of the key factors that cause road damage and affect road life and service capacity [1,2]. This factor is closely related to the structure, load, speed, and other factors of the vehicle [3,4]. Dynamic strain is a direct reflection of vehicle's dynamic load on the pavement structure and also an important mechanical index to characterize the service performance of asphalt pavement. The value of strain in

China's highway asphalt pavement design code is still based on the theory of a static elastic layered system. Although the fatigue cracking test used for the asphalt mixture layer adopts dynamic compression modulus correction at 20 °C, this test cannot truly reflect the dynamic characteristics of the pavement structure under loads and environmental conditions. Thus, it is necessary to systematically study the dynamic strain behavior characteristics of the asphalt pavement structural layer under the action of vehicle dynamic loads [5–7].

Accelerated pavement testing (APT) can quickly accumulate loads on test pavements to evaluate long-term pavement performance in a short period of time [8] and analyze the pavement's failure mechanism. Through sensitivity analysis [9], an APT project can promote the use of innovative building materials and methods, improve pavement design and analysis procedures, promote aging-pavement survey work, and accelerate loading tests, which are all considered to be effective means of studying dynamic strain characteristics caused by the dynamic loads and service performance of asphalt pavements [10–13]. Dong Zhonghong [14] used ALF (accelerated loading facility) to analyze the effects of lateral distribution, axle weight, and temperature on the dynamic response of asphalt pavement structures under the action of a single-shaft and double wheels. Guan Zhiguang [15] introduced the two factors of vehicle driving speed and tire pressure into a study on the dynamic responses of road surface structures and established a speed–axle weight regression model. Ye Yali [16] preliminarily studied the dynamic strain evolution law of flexible base asphalt pavement structures through an APT test road. Chen Jingyun [17] studied the mechanical response law of a typical asphalt pavement structural layer under a positive load and partial load of traffic based on MLS66. Wu Jinting [18] used a seismic wave modulus measuring instrument to analyze the instantaneous dynamic response of the bottom of the pavement structure layer under the experimental conditions of overweight and high frequency and analyzed the relationship between the number of loads and the cumulative strain of the asphalt surface layer.

Ozer [19] obtained the pavement structural layer response under two different loading states of pure shear and compression shear through indoor testing and analyzed the influence of vehicle load (load and tire inflation pressure) and maneuvering (braking, acceleration, and cornering) on the strain behavior of the pavement structural layer. Saleh [20] established a model between roughness and load repetition, axial load, and asphalt layer thickness, establishing a theoretical basis for studying the influence of vehicle power size on the dynamic characteristics of flexible pavement. Liu Dawei [21] established a three-dimensional finite element analysis model of semi-rigid pavement, which analyzed the effect of changes in vehicle driving speed on the dynamic damage of semi-rigid asphalt pavement. Navarrina [22] studied the changes to power-axle weight applied by heavy vehicles on the road surface over time by extending the quarter-car model and established a comprehensive model of flexible road fatigue analysis considering the impact of vehicle dynamic loads. Lu Zheng [23] and Chen Jingyun [24] established a dynamic analysis model of vehicle-uneven pavement-subgrade structure coupling, which was used to analyze the influence of multiple parameter coupling on road dynamic responses such as the driving speed, road surface unevenness, road thickness, tire stiffness, and base modulus. Huang Zhiyi [24] used the 3D-MOVE Analysis finite-layer software to analyze the dynamic strain characteristics of the structural layer of regenerated asphalt pavement under the action of moving a non-uniform distribution load. M.S.H. Al-Furjan has derived and solved the governing equations of structures using the differential quadrature method (DQM). Afterward, a parametric study is conducted to present the effects of SMA fiber. Due to the difference between the parameter material constitutive relationship and the content gradation and the actual asphalt mixture, it is difficult to accurately describe the fatigue performance by the finite element method and the differential quadrature method, and there are large errors. Since accelerated loading is the most advanced technical means to study the fatigue properties of asphalt, it can provide a more reasonable explanation for the complexity of the material properties of asphalt mixtures. Although domestic and foreign scholars have conducted a number of studies on the dynamic strain behavior of

asphalt pavement under the action of driving loads, foreign research has largely focused on flexible pavement. Consequently, the large differences in the pavement structure system decrease the applicability of foreign experimental research results. Moreover, due to the limitations of domestic accelerated loading equipment, funds, and technology, few scholars have conducted a complete study on the evolution of pavement strain behavior.

Plant-mixed hot recycling is one of the main means of producing reclaimed asphalt pavement, but RAP content, pavement structural stability, and durability have always restricted this type of pavement's wide application in China. Most scholars have only studied the strain behavior, dynamic characteristics, and long-term service performance of recycled asphalt pavement through theoretical analysis, material property testing, and numerical calculation methods, but no scholars have conducted a field-accelerated loading test on the omnidirectional strain response of the semi-rigid-base plant-mixed hot-recycled asphalt pavement structural system.

Based on these factors, we carried out an ALT acceleration loading test on an APT test road of the S222 West Lake Section of Rizhao City, Shandong Province, relying on the Applied Basic Research Project of the Ministry of Transport and the Transportation Science and Technology Project of Shandong Province. The bottom strain of the pavement structure in three different combinations was used as the experimental research object. We analyzed the evolution of the bottom-strain behavior of the plant-mixed hot-recycled asphalt pavement under the action of a high axle load, which provided a reference for studying the disease evolution mechanisms and long-term road performance of plant-mixed hot-recycled asphalt pavement.

2. Accelerated Loading Test Based on ALT

2.1. Test Equipment

The mobile road acceleration loading system, ALT, is shown in Figure 1. The equipment used was 26.342 m long, 4.220 m wide, and 7934 cm high. The hydraulic loading stepless adjustment system can apply single-sided single-axle or single-sided double-sided coupling loads. The double-sided wheelbase is 1.4 m, the effective load travel length is 10 m, the one-sided axle load range is 100–200 kN, and the one-way set wheel load can be applied 400–500 times per hour. The lateral offset load can be set, and the main and driven wheel double-axle double-wheel pack loading method is consistent with the actual road vehicle movement load state.

Figure 1. Mobile accelerated pavement loading equipment.

2.2. Road Surface Structure

A full-scale test road was paved at the S222 West Lake section of Rizhao City, Shandong Province, with a total length of 1200 m and a width of 10.5 m. This road is equipped with 3 kinds of pavement combination structures, where the surface layer is a typical 4 + 6 pavement structure, the base layer is cement-stabilized macadam, the thickness is 36 cm, and the bottom base layer is 18 cm low-dose cement-stabilized macadam. The rap

dosage in the SMA-13 plant-mixed hot-reclaimed asphalt mixture is 20%, and the RAP dosage in the AC-20 plant-mixed hot-reclaimed asphalt mixture is 40%. To conduct a comparative test, three of the combined forms of pavement (where the width of the test road is 3, 3, 3, and 3 m, the total length is 9 m, and the length is 3.75 m) was selected to accelerate loading under the same test environment. The specific road structure form is shown in Table 1.

Table 1. Types of road surface structures.

Structure A	Structure B	Structure C
4 cm AC-20 Hot-recycled asphalt concrete	4 cm SMA-13 Plain asphalt concrete	4 cm SMA-13 Plain asphalt concrete
6 cm AC-20 Hot-recycled asphalt concrete	6 cm AC-20 Hot-recycled asphalt concrete	6 cm AC-20 Plain asphalt concrete
18 cm Cement-Stabilized Macadam	18 cm Cement-Stabilized Macadam	18 cm Cement-Stabilized Macadam
18 cm Cement-Stabilized Macadam	18 cm Cement-Stabilized Macadam	18 cm Cement-Stabilized Macadam
18 cm Cement-Stabilized Macadam	18 cm Cement-Stabilized Macadam	18 cm Cement-Stabilized Macadam

2.3. Sensor Placement

To analyze the transverse and longitudinal strain behavior at the bottoms of the three different combinations of pavement layers during the accelerated loading process, a sensor was embedded at the bottom of the lower layer. The km-100 HAS-type buried strain sensor (TML Corporation, Tokyo, Japan) is equivalent to the modulus of the asphalt mixture using the intermediate axial rod and the asphalt mixture modulus of Japan. To prevent interference, the horizontal spacing of the sensor was set to 0.400 m, and the vertical spacing was 0.500 m. To truly record the vertical change law for the temperature field of the asphalt pavement structure, the vertical position of the test pavement was 0 cm. Thermocouple temperature sensors with an accuracy of up to 0.002 °C were buried at 4 and 10 cm. The specific temperature and strain transducer layout is shown in Figure 2.

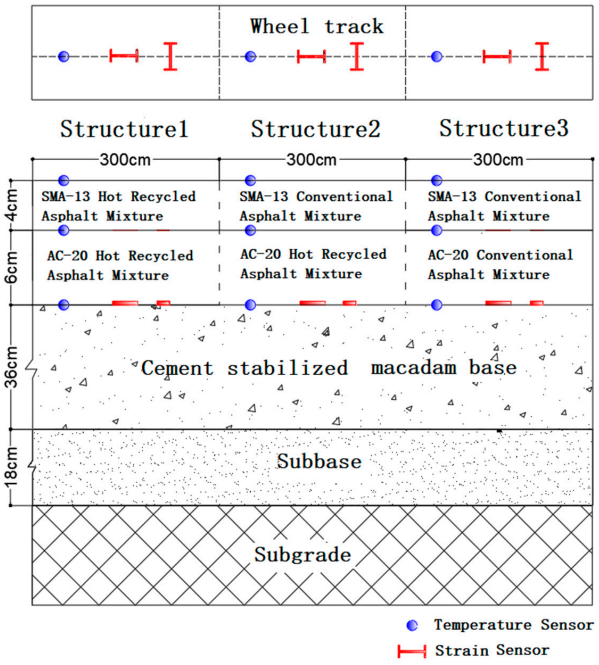

Figure 2. Schematic diagram of the test road sensor burial.

2.4. Implementation Program

This experimental study was carried out using a master–slave dual-axis accelerated loading system. The specific implementation setup for the accelerated loading test was as follows:

(1) Considering the difference in strain behavior under different axle weights, three axle weight classes were set up for comparison tests: 100, 130, and 150 kN.
(2) Considering the difference in strain behavior under different travel speeds, four speed classes were set: 12, 18, 22, and 24 km·h^{-1}.
(3) To test the long-term road performance of the plant-mixed hot-recycled asphalt pavement, the long-term loading test was set to 1.5 times the standard axle load, i.e., 150 kN, without considering the lateral offset moving load. The test environment was an open-air natural environment.
(4) Loading was performed 20 h/day for 60 days for a total of 400,000 times. The asphalt surface bottom layer tensile strain and asphalt surface layer permanent deformation were used as the test index and converted to a cumulative 5.5 million standard axle load.
(5) The base strain and pavement temperature gradient were continuously collected in real time, where the layer substrate strain acquisition frequency was 100 Hz, and the temperature gradient acquisition frequency was 10 Hz.

3. Analysis of Test Results

3.1. Determination of the Most Unfavorable Location for the Load

The dynamic load generated by driving a vehicle will act on the road surface, thereby affecting the road. It is beneficial to determine the most unfavorable position of the load to better study the pavement failure mode and improve road surface design. Therefore, we carried out a strain test under the center and side tracks of the gear train on a previous indoor full-scale test road. The sensor data from the two cases were then compared and analyzed, as shown in Table 2.

Table 2. The longitudinal strain at different position of the wheel bottom.

Sensor Number	Location	Longitudinal Tensile Strain /× 10^{-6}	Longitudinal Compressive Strain/× 10^{-6}	Total Amplitude /× 10^{-6}
11# sensor (Early foundation)	Under the center of the wheel gap	47.8	−3.4	51.2
	Under unilateral wheel tracks	96.3	−12.2	108.5
31# sensor (Early foundation)	Under the center of the wheel gap	44.2	−22.4	66.6
	Under unilateral wheel tracks	47.4	−49.0	96.4

As can be seen from Table 2, the amplitude of longitudinal tensile strain, compressive strain, and total strain under a single-wheel track in the case of two axles and two wheels are all greater than the values under the center of the wheel gap, so the degree of failure under a single-wheel track is much greater than that under the center of the wheel train. Therefore, the loading position of the embedded strain sensor is directly below the center of the single-wheel track.

3.2. Influence of Number of Axles

The acceleration loading equipment used at home and abroad is mainly of the single-axle double-wheel type. We adopted double-axle double-wheel-type acceleration loading equipment and analyzed the transverse and longitudinal bottom-strain test data of structure 3 at 13:00 on 21 August, as shown in Figure 3.

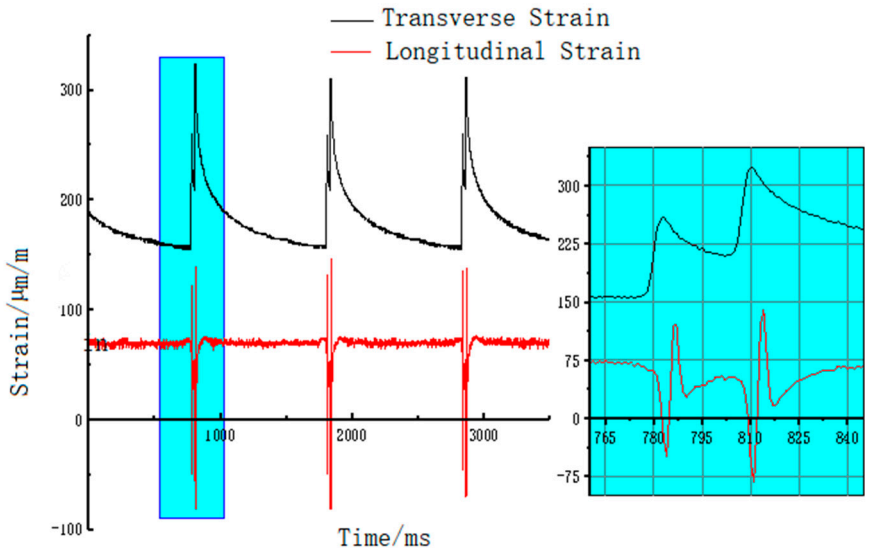

Figure 3. Transverse longitudinal strain at the base of the layer under biaxial action.

Figure 3 demonstrates the following:

(1) The transverse tensile strain value of the pavement is always positive, and the longitudinal tensile strain is alternately positive and negative. This phenomenon occurs mainly because the transverse strain gauge always experiences tension under the vertical action of the wheel load, the longitudinal strain gauge is subjected to horizontal and vertical combined loads, and the strain value alternates between positive and negative. When the tire is close to the strain timing, the horizontal and lateral components of the wheel load act on the longitudinal strain gauge, and the strain is negative. When the wheel load acts directly above the longitudinal strain gauge, the strain gauge is completely subjected to a vertical load, and the strain is positive.

(2) There are two peaks and troughs in the transverse and longitudinal strain data. Taking the transverse strain as the calculation object, the difference between the second peak and the first peak is 60~70 μm/m. Taking the longitudinal strain as the calculation object, the difference between the first wave crest and the second wave crest is 15~20 μm/m, and the difference between the second wave trough and the first wave trough is 40~45 μm/m. Asphalt mixture is a viscoelastic body, which will show elastic properties under the action of instantaneous load. Due to the deformation hysteresis effect caused by its viscoelastic characteristics, the strain generated by the first axle cannot be fully released, and the second axle produces strain superposition. Therefore, the dynamic effect of a biaxial load on pavement is much larger than that of a uniaxial load. Existing design codes still use the static load of a single-axle double-wheel set for the load, which is quite different from the actual multi-axle dynamic load of existing vehicles, which needs further study.

(3) The longitudinal strain reflects the complex stress state of the road surface under the action of the wheel load. The longitudinal compressive strain of the bottom layer is not significantly different from the lateral tensile strain, and the longitudinal tensile strain of the bottom layer is greater than the lateral tensile strain. The actual longitudinal stress on the bottom of the pavement is a variable strain state of alternating compression–tension–compression. Therefore, when designing asphalt pavement, the tensile and compressive strain and strain amplitude of the bottom layer should be considered.

3.3. Influence of Axle Weight

To analyze the effect of axle weight on the dynamic response of the pavement structure, the test data of longitudinal tensile strain and transverse tensile strain at the bottom of the three pavement layers at 08:00 on 21 August were selected for analysis, as shown in Table 3.

Table 3. Dynamic responses of layer substrates under different loads.

Pavement Structure	Longitudinal Tensile Strain/$\times 10^{-6}$			Longitudinal Compressive Strain/$\times 10^{-6}$			Transverse Tensile Strain/$\times 10^{-6}$		
	100 kN	130 kN	150 kN	100 kN	130 kN	150 kN	100 kN	130 kN	150 kN
Structure 1	76.9	82.6	87.2	−90.5	−99.0	−105.4	132.1	142.3	150.0
Structure 2	76.1	82.0	86.8	−87.5	−97.0	−103.3	132.4	141.6	149.3
Structure 3	78.3	84.3	89.7	−90.1	−100.3	−107.8	133.5	143.2	151.8

The following can be seen in Table 3:

(1) When the axle load increases by 30% and 50%, the longitudinal tensile strain of structure 1 increases by 7.41% and 13.39%, the longitudinal compressive strain increases by 9.39% and 16.46%, and the lateral tensile strain increases by 7.72% and 13.55%, respectively. The longitudinal tensile strain of structure 2 increases by 7.75% and 14.06%, the longitudinal compressive strain increases by 10.86% and 18.06%, and the transverse tensile strain increases by 6.95% and 12.76%, respectively. Finally, the longitudinal tensile strain of structure 3 increases by 7.66% and 14.56%, the longitudinal compressive strain increases by 11.32% and 19.64%, and the lateral tensile strain increases by 7.27% and 13.71%, respectively. The growth of underlayer strain is much less than that of the axial load, and the relationship between the underlayer strain and axial load is nonlinear.

(2) Under the same environment and different axle loads, the three kinds of pavement structures have small differences in their bottom strain, indicating that the pavement performance of the high-volume recycled asphalt pavement studied in this paper can basically achieve the new asphalt pavement standards.

During the test, to deeply study the nonlinear relationship between the axle load and bottom strain, the tire contact area under different axle loads (100, 130, and 150 kN) was tested on the spot using blue paint and white coordinate grid paper. We also measured and calculated the ground pressure (see Table 4 and Figure 4 for details).

Table 4. Wheel ground area under different ground areas.

Axial Load/kN	Single Wheel Ground Area/cm^2	Grounding Pressure/Mpa
100	304.87	0.82
130	318.63	1.02
150	353.77	1.06

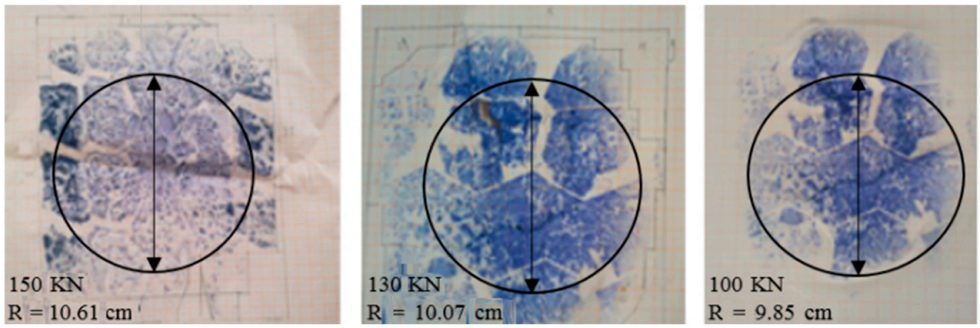

Figure 4. Diagram of wheel ground area.

It can be seen from Table 4 and Figure 4 that with an increase in the axle load of the vehicle, the contact area of the tire increases nonlinearly, and the contact pressure also increases nonlinearly. Therefore, the ground contact pressure can be used as an evaluation index to analyze the influence of overloaded vehicles on the road surface.

3.4. Influence of Temperature

To investigate the effect of temperature on the bottom strain of recycled asphalt pavement, accelerated loading tests were carried out at multiple temperature levels, and the laws of transverse maximum tensile strain and longitudinal maximum tensile strain for the bottom layer under different temperature conditions were analyzed. The driving speed of the vehicle was 24 km·h^{-1}, the axle load was set to 150 kN, and the tire pressure was 1.02 Mpa.

3.4.1. Analysis of Temperature Heat Transfer in Asphalt Pavements

In this paper, test data of Rizhao area in Shandong Province, taken during the high-temperature period from July to November, were used as an example to conduct the study. To intuitively observe the road temperature gradient and environmental temperature distribution, the temperatures during a representative high-temperature period (from 1 September to 22 September) were selected.

Figure 5 shows the temperature and ambient temperature distributions at different depths of asphalt pavement in structure 3. The variation rule of road surface temperature and ambient temperature is basically the same. With an increase in measuring-point depth, the road surface temperature experiences a certain lag with ambient temperature. The deeper the depth is, the more obvious the lag becomes, indicating that the road surface temperature and ambient temperature have obvious nonlinear characteristics.

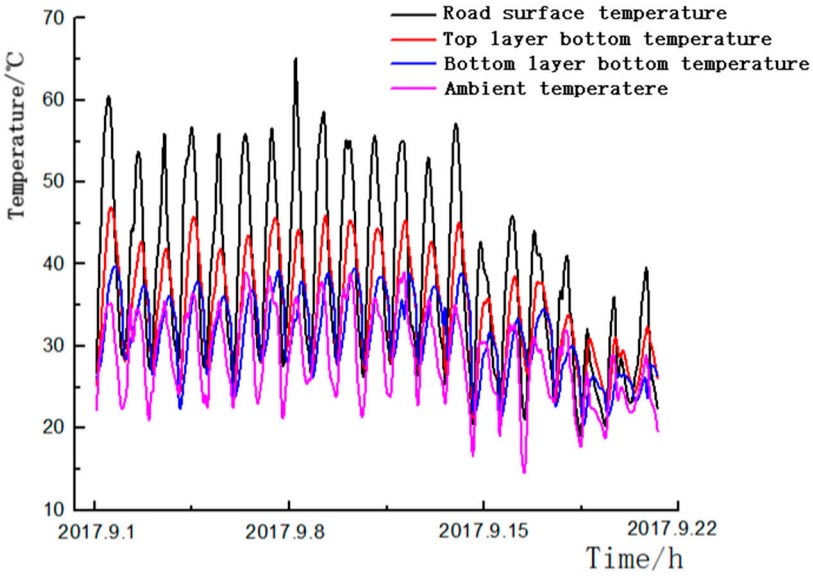

Figure 5. Measured ambient and pavement temperature data.

In this study, we used the temperature gradient calculation formula:

$$G = \frac{T_1 - T_2}{|y_1 - y_2|} \times 1000 \quad (1)$$

where G is the temperature gradient, °C/m; T_i is the temperature in the vertical direction y_i, °C; and y_i is the vertical distance of the i-th test point, mm.

Using to Formula (1), we carried out temperature gradient calculations on the temperature monitoring data from the three kinds of pavement structures. The maximum positive temperature gradient refers to the maximum positive temperature difference formed by the road surface temperature and the bottom layer temperature. The maximum positive temperature gradients of the three pavement structures were 359, 325, and 314 °C/m. The maximum positive temperature gradient occurred at 13:00 on 9 September when the weather was clear and the cloudiness was low. The ambient temperature was 36.3 °C; the

surface temperature of the road surface was as high as 69.3 ± 1 °C under the action of strong infrared rays; the temperature of the upper bottom layer was 41.4, 41.5, and 41.8 °C; the bottom layer temperature was 34.4, 34.5, and 35.0 °C. Structure 2 and structure 3 had the same top layer material, and the temperature of the top bottom layer was basically the same. Structure 1 was 0.6 °C lower than the bottom layer temperature of structure 3. The test results show that the pavement used in structure 1 has poor heat transfer. This phenomenon is due to the presence of significant amounts of colloid, asphaltene, and other materials in the recycled asphalt mixture, which together reduce the heat transfer efficiency of the pavement.

3.4.2. Effect of Temperature on the Strain Behavior of the Layer Substrate

On September 18, the weather in Rizhao City was sunny and windy. The bottom temperatures and road surface temperatures of the three kinds of pavement structures, collected from 7:00 to 21:00, were compared and analyzed with the horizontal and vertical maximum strain data of the bottom layer. Specific data are shown in Figures 6–8.

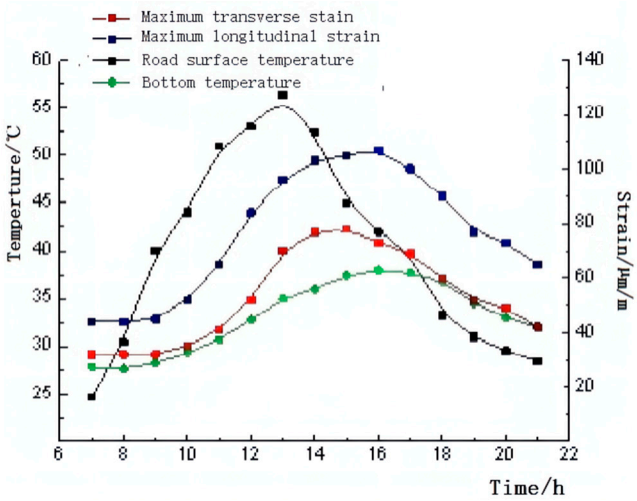

Figure 6. Structure A temperature versus maximum tensile strain in the transverse and longitudinal direction at the base of the layer.

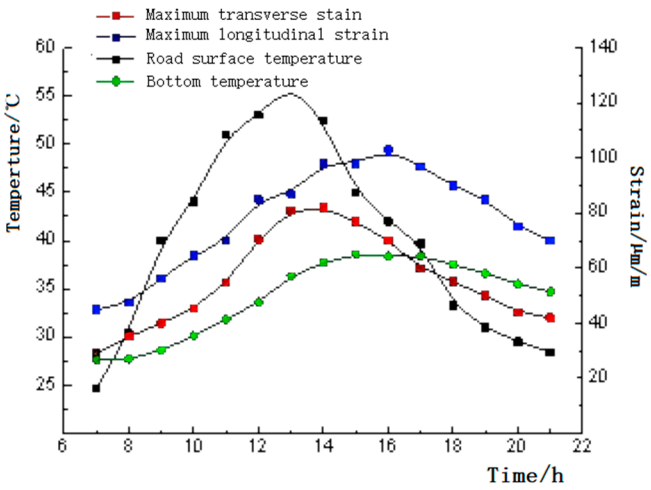

Figure 7. Structure B temperature versus maximum transverse and longitudinal tensile strain at the base of the layer.

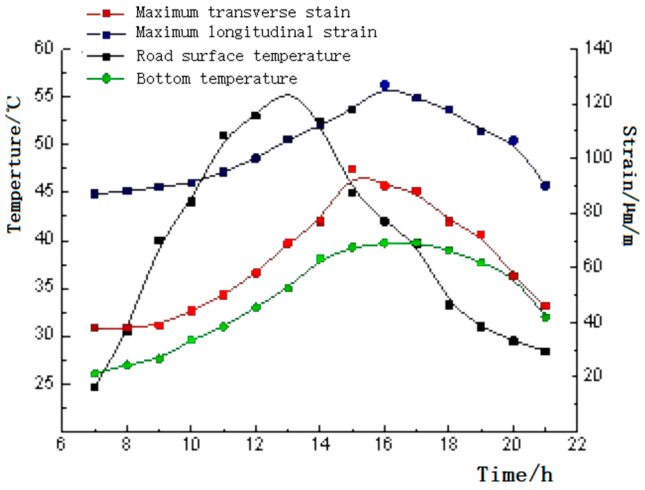

Figure 8. Structure C temperature versus transverse and longitudinal tensile strain at the base of the layer.

The following can be seen in Figures 6–8:

(1) The longitudinal and transverse tensile strains of the three pavement structures are basically consistent with the variation of the temperature at the bottom of the pavement. When the temperature at the bottom increases, the strain increases, and when the temperature decreases, the strain decreases. In Figure 6, we see that the layer bottom temperature, the maximum transverse strain, and the maximum longitudinal should reach a maximum value for structure A about an hour later than the road surface temperature; in Figure 7, in the time range 12–14, the road surface temperature is the highest, and the maximum transverse strain is more sensitive to the change in temperature, while the changes in the bottom temperature and the maximum longitudinal strain with temperature are slightly delayed, and the strain reaches the maximum value around 16 o'clock; the change in Figure 8 is closer to that in Figure 6.

(2) Under the same temperature conditions, the longitudinal tensile strain at the bottom of the three pavement structures is greater than the transverse tensile strain; under high temperature conditions, the longitudinal tensile strain is about 1.0–1.5 times the transverse tensile strain, so transverse fatigue cracking of the pavement bottom layer is the first to appear.

(3) At high temperatures, the bottom strain of structure C is obviously larger than that of structure A and B, with little difference between the bottom strain of structure A and B. Structure C belongs to new asphalt pavement, which has good heat transfer, good viscoelasticity of pavement materials, and a large bottom response. The reclaimed pavement has better high-temperature performance than the new pavement. At room temperature, the bottom temperatures of the three pavement structures are close to each other, but there is little difference in the bottom strain values.

(4) Under the action of repeated axial loads on the road surface, the cracks at the bottom of the layer cannot be directly reflected on the road surface. With the help of the highly consistent relationship between the temperature of the bottom of the layer and the longitudinal tensile strain, the cracks at the bottom of the layer can be analyzed. This analysis is used for road performance inspections and disease control. Assessment provides a new approach.

3.5. Effect of Vehicle Speed

First, we analyzed the relationship between the vehicle speed and the bottom strain of the asphalt pavement at 14:00 on 21 August, when the driving equipment was accelerated and loaded at 12, 18, 22, and 24 km·h^{-1}. Three kinds of lateral and longitudinal strains were collected from the pavement bottom layer during driving for comparative analysis. In this

paper, the lateral and longitudinal tensile strains of the pavement bottom layer of structure A under four driving speeds were taken as an example, as shown in Figures 9 and 10.

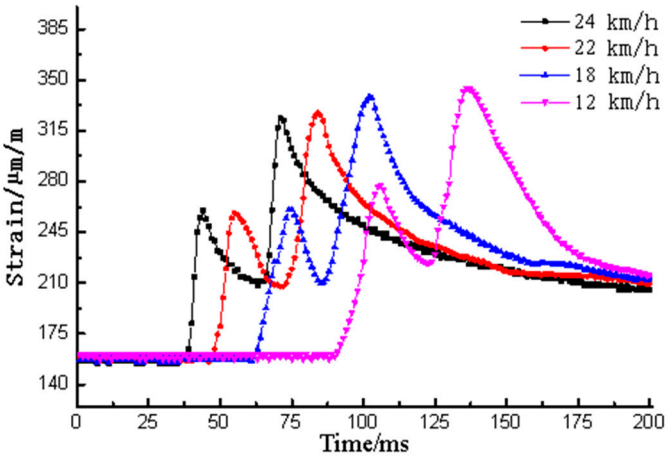

Figure 9. Relationship between vehicle speed and maximum transverse tensile strain at the base of the layer.

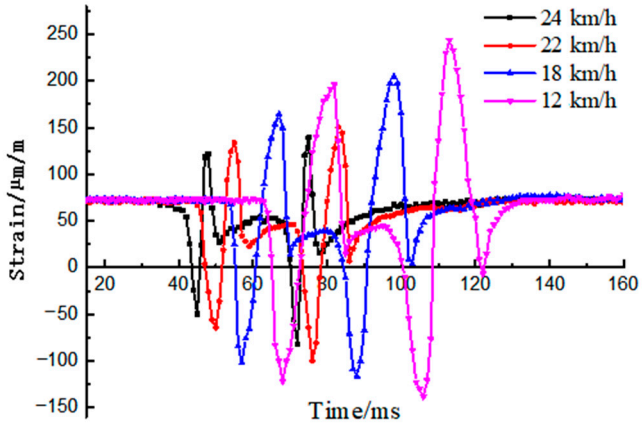

Figure 10. Relationship between vehicle speed and maximum longitudinal tensile strain at the base of the layer.

It can be seen from Figures 9 and 10 that the driving speed of the driving equipment directly affects the wheel load action time and the strain pulse time. As the viscoelastic material of asphalt mixture increases, so too does the vehicle travel speed (relative to the load action frequency). Moreover, the greater the modulus, the lower the strain value at the bottom of the layer.

According to the test data of structures B and C, there is little difference in the bottom strain value between the recycled asphalt pavement and the new asphalt pavement under the same driving speed conditions. The bottom strain values of the three pavement structures all decrease with an increase in the driving speed of the driving equipment, and this trend is consistent. It can be demonstrated that the initial material modulus of the recycled asphalt pavement is close to the modulus of the new asphalt pavement. This conclusion was also confirmed in the previous laboratory tests.

With an increase in vehicle driving degree, the maximum lateral and longitudinal strains of the bottom layer gradually decrease, and the trend of strain reduction does not decelerate. If the driving speed of the driving equipment continues to increase, the bottom layer strain value will reach a relatively stable value. According to the test results, a

calculation model for the maximum strain value of structure A (12 km/h ≤ v ≤ 24 km/h) can be established:

$$\varepsilon = 368.5e^{-0.05v} \quad (2)$$

According to the measured data of the Jinan South Ring Expressway field test road (same road structure) paved by the research team, when the heavy-duty vehicle travelled at a speed of 80~120 km/h, the maximum strain value of the bottom layer was 239.3×10^{-6}~206.2×10^{-6}, and the error between the measured value and the calculated value was within 5.0%. The calculation models for different pavement structures and axle loads were established through accelerated loading test data corresponding to the test parameters.

3.6. Influence of the Number of Load Actions

The relationship between the number of loads and the cumulative bottom strain was also analyzed. As an example, we compared and analyzed the lateral and longitudinal cumulative tensile strains of pavement structure A and the number of loads. The relationship between the cumulative tensile strain and the number of loads is shown in Figure 11.

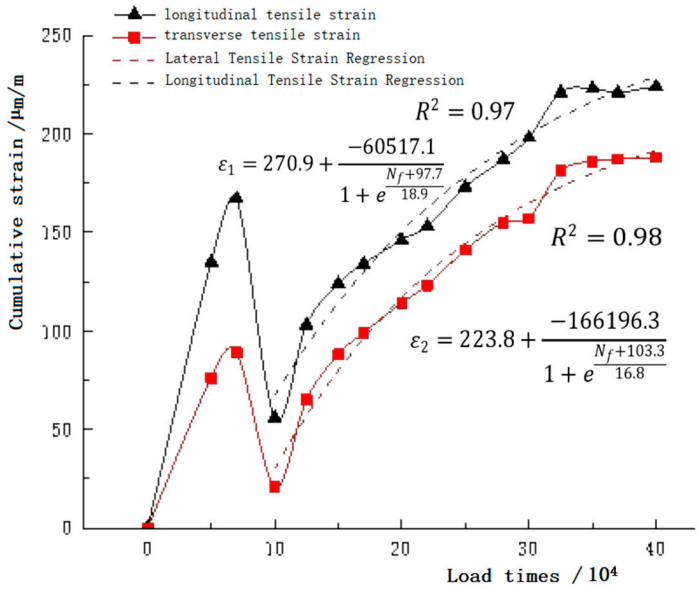

Figure 11. Cumulative strain versus number of load actions.

It can be seen from Figure 11 that in the initial stage of loading, the lateral and longitudinal cumulative strains at the bottom of each layer rise sharply, and the initial cumulative strain is about 75.0% of the total cumulative strain. With an increase in the number of loadings, the increasing trend of the strain decelerates. The cumulative longitudinal and transverse tensile strains tended to be stable when loaded 310,000 times, and the thermally recycled asphalt mixture entered the compaction stage. The average rut at this time was 1.30 cm, and the average rut at the end of the test was 1.55 cm.

According to the comparative analysis of Figures 9–11, the instantaneous strain is sometimes greater than the cumulative strain, indicating that hot-recycled asphalt pavement had self-healing abilities during the test process and in the intermittent stage. Thus, the number of loads here is not directly related to the instantaneous strain but directly related to the cumulative strain. The cumulative strain prediction model based on the Boltzmann function can better reflect the relationship between the cumulative strain at the bottom of the layer and the number of load actions, as shown in Equations (3) and (4):

$$\varepsilon_1 = 270.9 + \frac{-60517.1}{1 + e^{\frac{N_f + 97.7}{18.9}}} \quad (3)$$

$$\varepsilon_2 = 223.8 + \frac{-166196.3}{1 + e^{\frac{N_f + 103.3}{16.8}}} \quad (4)$$

The reason for the sharp decline stage shown in Figure 11 is that the bottom deformation was recovered after the test was interrupted for 6 days due to weather reasons and equipment failure. The test data indicate that the longitudinal accumulated strain recovered by 66.5%, and the lateral accumulated strain recovered by 76.4%, indicating that the thermal regenerative asphalt pavement had a strong ability to recover initial deformation.

4. Concluding Remarks

(1) In the case of dual axles and two wheels, the strain amplitude of the asphalt pavement under the center of the wheel track on one side was larger than that under the center of the wheel gap, and the load on the asphalt pavement under the center of the wheel track on one side was higher than that under the center of the wheel gap.

(2) The damage effect of a single dual-axle wheel load was far greater than that of the two single-axle wheel loads. The longitudinal strain at the bottom of the pavement layer always maintained an alternating state of compression–tension–compression, and the longitudinal tensile strain at the bottom of the pavement layer was always greater than the lateral tensile strain. Moreover, transverse fatigue cracks appeared first. Under high temperature conditions, the longitudinal tensile strain was about 1–1.5 times the transverse tensile strain.

(3) When the axle load increased by 30% and 50%, the longitudinal tensile strain increased by 7.41–14.56%, respectively; the longitudinal compressive strain increased by 9.39–19.64%; and the transverse tensile strain increased by 7.72–13.71%. The bottom strain of asphalt pavement had a nonlinear relationship with the axle load and a linear relationship with the ground pressure.

(4) The maximum positive temperature gradient of structure A was 12.50% higher than that of structure B and 9.50% higher than that of structure C. The heat transfer efficiency of the thermally recycled pavement was lower than that of the new asphalt pavement, and the temperature had a greater impact on the bottom strain of the asphalt pavement.

(5) The driving speed directly affects the load action time and pulse time of the response. The higher the vehicle speed was, the smaller the bottom layer strain value became. Based on the accelerated loading test data, a prediction model for the maximum bottom layer strain was established. The error rate in the calculations of the maximum strain value of the pavement bottom layer was controlled within 5%.

(6) No direct relationship was observed between the loading times and instantaneous strain, and the relationship between the loading times and accumulative bottom could be represented using the Boltzmann function. After 310,000 loads, the hot-recycled asphalt pavement entered the dense stage, and plastic deformation was basically completed. Under a load of 400,000 times, there was no obvious difference in rut performance between the recycled asphalt pavement and the new asphalt pavement.

(7) Certain limitations remain in evaluating the performance of hot-recycled asphalt pavement based on the bottom-strain behavior of asphalt pavement. The mechanical response of high-volume thermally recycled pavement can basically fulfill the new pavement standards, but the uniformity and migration law of thermally recycled materials cannot be determined in the strain behavior clearly and must be further verified in combination with the properties of thermally recycled materials.

(8) Based on the above conclusions, this paper accelerates road damage through the fast loading method of controllable axle load, and provides a real data model for analyzing the influence of various factors such as road load on the strain. Considering the actual operating conditions on the road, the poor accuracy, authenticity, practicability and real-time performance of the experimental data, and the resulting errors in the analysis results, the accelerated loading test is a cost-effective method. In addition, the dynamic strain behavior analysis of asphalt pavement also plays a very important

role in the study of pavement failure modes. Therefore, the popularization and application of the pavement accelerated loading test system is of great practical significance to study the long-term performance of the pavement. In this paper, the ALT biaxial accelerated loading test equipment is used to simulate the dynamic load of the vehicle, and the parameters such as axle load, temperature, speed, and loading times are synthesized, and the development law of the bottom strain of the three kinds of pavement structures is analyzed, which will also provide information for the advancement of related research.

Author Contributions: Conceptualization, J.L.; methodology, J.L. and Y.L.; software, J.L. and Y.L.; validation, H.Z.; formal analysis, H.Z.; investigation, H.Z.; resources, J.L. and S.Z.; data curation, J.L. and H.Z.; writing—original draft preparation, J.L. and H.Z.; writing—review and editing, J.L. and H.Z.; supervision, J.L. and P.L.; project administration, J.L., C.X. and P.A.; funding acquisition, J.L. and C.X. All authors have read and agreed to the published version of the manuscript.

Funding: Shandong Transportation Science and Technology Project: Preparation and road performance of REOB/SBS composite modified asphalt (2021B11).

Institutional Review Board Statement: Not applicable.

Informed Consent Statement: Not applicable.

Data Availability Statement: The experimental data in this paper are from the pavement material laboratory of Shandong Jiaotong University, which is the provincial key laboratory.

Conflicts of Interest: The authors declare that they have no conflict of interest regarding the publication of this paper.

References

1. Pan, T.C.; Li, J. Dynamic vehicle element method for transient response of coupled vehicle-structure systems. *J. Struct. Eng.* **2002**, *128*, 214–223. [CrossRef]
2. Watts, G.R.; Krylov, V.V. Ground-borne vibration generated by vehicles crossing road humps and speed control cushions. *Appl. Acoust.* **2000**, *59*, 221–236. [CrossRef]
3. Bilodeau, J.P.; Gagnon, L.; Doré, G. Assessment of the relationship between the international roughness index and dynamic loading of heavy vehicles. *Int. J. Pavement Eng.* **2017**, *18*, 693–701. [CrossRef]
4. Navarrina, F.; Ramírez, L.; París, J.; Nogueira, X.; Colominas, I.; Casteleiro, M.; Fernández-de-Mesa, J.R. Comprehensive model for fatigue analysis of flexible pavements considering effects of dynamic axle loads. *Transp. Res. Rec.* **2015**, *2524*, 110–118. [CrossRef]
5. Zhuang, C.Y.; Ye, Y.; Zhang, N. Analysis of dynamic response of semi-rigid base asphalt pavement based on APT test. *J. Shandong Transp. Inst.* **2014**, *22*, 55–61.
6. Lv, S.; Chen, J. Study on the decay law of asphalt mixture stiffness based on accelerated loading test. *J. Highw. Transp. Res. Dev.* **2016**, *33*, 1–6.
7. Hu, P.; Liu, Z.J. Analysis of fatigue damage of asphalt pavement under accelerated loading conditions. *J. Shandong Traffic Coll.* **2010**, *18*, 74–77.
8. Embacher, R.A.; Snyder, M.B.; Odden, T.D. *Using the Minnesota Accelerated Loading Facility to Test Retrofit Dowel Load Transfer Systems*; Transportation Research Record No. 1769; National Academy Press: Washington, DC, USA, 2001; Volume 1769, pp. 134–141.
9. Plessis, D.; Nokes, L.; Mahdavi, W.A.; Burmas, N.; Holland, J.; Lee, E.B. *Economic Benefits Assessment of Accelerated Pavement Testing Research in California: Case Study*; Transportation Research Record No. 2225; Research Board of the National Academies: Washington, DC, USA, 2011; Volume 2225, pp. 137–146.
10. Xu, Q. Accelerated loading test study of semi-rigid base and flexible base asphalt pavement. *Highw. Traffic Technol.* **2011**, *7*, 115–119.
11. Meng, S. Accelerated loading test study on the performance of semi-rigid base asphalt pavement. *Highw. Traffic Technol.* **1997**, 61–66.
12. Jiang, H.; Bian, X.; Chen, Y. Full-scale accelerated loading test for high-speed railway track-roadbed train moving load simulation. *J. Civ. Eng.* **2015**, *48*, 85–95.
13. Ran, W.; Ling, J.; Zhao, H. Accelerated loading dynamic response of epoxy asphalt pavement at high temperature and footage. *J. Tongji Univ.* **2015**, *43*, 1823–1828.
14. Dong, Z.H.; Xu, Q.L.; Lv, P.M. Dynamic response of semi-rigid base asphalt pavement based on accelerated loading test. *Chin. J. Highw.* **2011**, *24*, 1–5.
15. Guan, Z.-G.; Zhuang, C.-Y.; Lin, X.-X. Accelerated loading dynamic response of footprint asphalt concrete pavement. *J. Transp. Eng.* **2012**, *12*, 24–31.
16. Ye, Y.; Zhuang, C.; Wang, L.; Song, X.J. Dynamic response of flexible base asphalt concrete pavement based on accelerated loading test. *Highways* **2013**, *58*, 1–7.

17. Chen, J.Y.; Liu, J.Y.; Liu, Y.Q. Dynamic response of asphalt pavement structures under accelerated loading conditions. *J. Harbin Eng. Univ.* **2014**, *35*, 771–776.
18. Wu, J.T.; Ye, F. Analysis of strain behavior of asphalt pavement under heavy-frequency loading of MLS66. *Chin. J. Highw.* **2014**, *27*, 9–16.
19. Ozer, H.; Al-Qadi, I.L.; Hasiba, K.I.; Wang, H. Pavement layer interface shear strength using a hyperbolic Mohr-Coulomb model and finite element analysis. Airfield and Highway Pavement 2013: Sustainable and Efficient Pavements. In Proceedings of the Airfield & Highway Pavement Conference, Los Angeles, CA, USA, 9–13 June 2013; American Society of Civil Engineers: Los Angeles, CA, USA, 2013; pp. 1445–1456.
20. Saleh, M.F.; Owusu-Antwi, M. Mechanistic roughness model based on vehicle-pavement interaction. *Transp. Res. Rec.* **2000**, *1699*, 114–120. [CrossRef]
21. Liu, D.A.W.; Chen, J.; Huo, W. Research on the damage of road surface by vehicle speed. *J. Agric. Mach.* **2003**, *1*, 11–13.
22. Lu, Z.; Yao, H.L.; Hu, Z. Dynamic response analysis of uneven pavement based on coupled vehicle-road structure vibration. *J. Geotech. Eng.* **2013**, *35*, 232–238.
23. Chen, J.Y.; Sun, Y.I.R. Dynamic response analysis of a coupled vehicle-road system based on contact nonlinearity. *Vib. Shock.* **2013**, *32*, 119–124.
24. Huang, Z.; Chen, Y.; Zhang, Q. Response analysis of hot recycled asphalt pavement under moving load. *J. Railw. Sci. Eng.* **2019**, *16*, 107–113.